
GRAFT: Auditing Graph Neural Networks via Global Feature Attribution

Rishi Raj Sahoo^{1,2} Subhankar Mishra^{1,2}

¹National Institute of Science Education and Research (NISER), Bhubaneswar, India

²Homi Bhabha National Institute, Mumbai, India
 {rishiraj.sahoo, smishra}@niser.ac.in

Abstract

Graph Neural Networks (GNNs) achieve strong performance on node classification tasks but remain difficult to interpret, particularly with respect to *which input features* drive their predictions. Existing global GNN explainers operate at the *structural* level identifying recurring subgraph motifs, but none explain model behaviour *globally* at the level of input node attributes. We propose GRAFT, a post-hoc global explanation framework that identifies class-level feature importance profiles for GNNs. The method combines diversity-guided exemplar selection, Integrated Gradients-based attribution, and aggregation to construct a global view of feature influence for each class, which can be further expressed as concise natural language rules using a large language model with self-refinement. We evaluate GRAFT across multiple datasets, architectures, and experimental settings, demonstrating its effectiveness in capturing model-relevant features, supporting bias analysis, and enabling feature-efficient transfer learning. In addition, we introduce a structured human evaluation protocol to assess the interpretability of generated rules along dimensions such as accuracy and usefulness. Our results suggest that GRAFT provides a practical and interpretable approach for analysing feature-level behaviour in GNNs, bridging quantitative attribution with human-understandable explanations.

1 Introduction

Graph Neural Networks achieve state-of-the-art accuracy on node classification across citation networks, co-authorship graphs, product graphs, and social networks [1, 2, 3, 4]. Yet their predictions remain largely opaque. A practitioner cannot easily answer: *which node attributes drive the model’s class decisions?* This opacity is not merely inconvenient: a GNN trained for citation classification may exploit irrelevant author-name tokens, or a product-recommendation model may rely on price artefacts injected at training time. Without a way to audit *which features a GNN actually uses for each class*, such shortcuts go undetected until deployment.

Model auditing gap. We propose *feature shortcut detection* as the primary evaluation target for global GNN explainers. Given a trained GNN, does the explainer identify features the model relies on, rather than features merely correlated with class labels in the training set? We formalise this through controlled bias-injection experiments: a synthetic binary feature is correlated with a target class and injected into the graph; a trustworthy explainer must surface this feature prominently. No existing global GNN explainer has demonstrated this capability.

This work. We fill the global feature-level explainability gap with GRAFT (Global gRaph Attribute Feature aTtribution), a post-hoc, model-agnostic method that works with any GNN producing node embeddings. The pipeline has four stages as illustrated in Figure 1: (1) select k maximally diverse

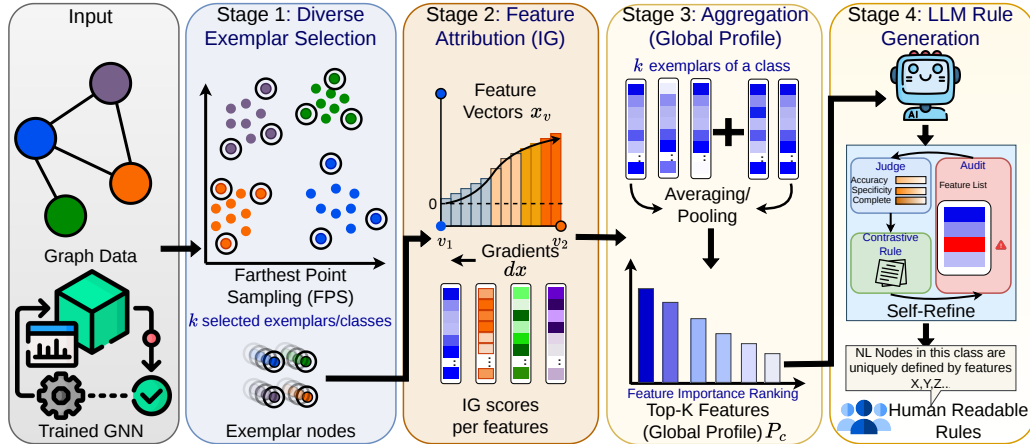


Figure 1: GRAFT pipeline. **Input:** trained GNN f and graph (G, X) . **Stage 1** selects k diverse exemplar nodes per class via Farthest Point Sampling in embedding space. **Stage 2** computes Integrated Gradients for each exemplar: a zero baseline, 50 Riemann interpolation steps, yielding $IG_e \in \mathbb{R}^d$. **Stage 3** aggregates $|IG|$ over exemplars and ranks features by mean importance, producing class profile \mathcal{P}_c . **Stage 4** verbalises \mathcal{P}_c as a natural language rule r_c via an LLM with self-refinement, which is human-readable.

class-representative nodes via Farthest Point Sampling; (2) compute Integrated Gradients [5] per exemplar; (3) aggregate attributions into a ranked class-level feature importance profile; and (4) verbalise the profile as natural language rules via an LLM. GNN explainability methods split along locality (local vs. global) and granularity (structural vs. feature-level) axes. Global structural methods now exist: GNNXEMPLAR [6] identifies representative subgraph patterns per class; CIFlow-GNN [7] uses causal flows over graph topology. The *global feature-level* quadrant is unoccupied; GRAFT fills it.

Beyond profiles, we introduce three analysis tools: (i) *Cross-architecture consensus*: what fraction of top- K features are identified independently by ≥ 3 of 4 architectures? (ii) *Contrastive profiles*: for class c , which features have high importance for c but not for any other class? (iii) *Jaccard stability*: how reproducible is the top- K feature set across seeds?

Contributions.

1. **Auditing application:** the first demonstration of feature shortcut detection for GNNs via global attribution: injected spurious features are recovered within top-3 across all 11 (dataset, architecture) pairs tested (GCN and GAT architectures; §4.2), rank 1 in 9 of 11.
2. **Method:** GRAFT, the first global, feature-level, post-hoc GNN explainer with natural language rule generation (§3).
3. **Discriminative evaluation:** GRAFT-selected features (1%–17% of the feature space on the evaluated benchmarks) achieve competitive transfer performance, outperforming frequency-based selection on several datasets while remaining comparable on others (§4.3).
4. **Systematic evaluation:** 260 runs across 13 datasets, 4 architectures, 5 seeds; three novel analysis tools quantify explanation quality beyond fidelity.

2 Related Work

Local GNN explainability. GNNExplainer [8] learns per-instance edge/feature masks; PGExplainer [9] parametrises masks for generalisation. Both target individual predictions; their outputs cannot be straightforwardly aggregated to class-level feature attributions. Per-node Integrated Gradients and SHAP [10] produce scalar feature attributions for each node, but a class-level summary requires choosing which nodes to include and how to pool, choices that are ad-hoc and that strongly

affect the result. *From Nodes to Narratives* [11] generates LLM-based natural language explanations at the per-node (local) level.

Global GNN explainability. GNNXEMPLAR [6] is the closest prior work: it selects structural exemplars and uses an LLM to describe recurring subgraph patterns. Its attribution target is graph structure; no feature importance profile is produced. CIFlow-GNN [7] identifies globally influential structural components via causal intervention flows. Global Shapley methods [12] attribute importance to activation patterns in intermediate layers rather than raw input features. GRAFT is complementary to GNNXEMPLAR: the two methods can be combined ("GRAFT+", see §5) to produce explanations covering both structural and feature-level aspects of a class. Table 1 summarises the landscape.

Table 1: Comparison of global GNN explanation methods. GRAFT uniquely combines global scope, input-feature attribution, and NL rules.

Method	Global?	Feature-level?	NL rules?
GNNExplainer [8]	×	✓(local)	×
GNNXEMPLAR [6]	✓	×(structural)	✓
CIFlow-GNN [7]	✓	×(structural)	×
From Nodes to Narratives [11]	×	✓(local)	✓
Shapley for GNNs [12]	✓	Partial (activations)	×
GRAFT (ours)	✓	✓	✓

Feature attribution. Integrated Gradients [5] satisfies completeness (attributions sum to $f(x) - f(\mathbf{0})$) and sensitivity (features affecting output receive non-zero attribution). GRAFT uses IG as a sub-routine; any scalar-per-feature attribution method (Grad×Input [13], SHAP [10]) can be substituted.

Exemplar-based explanations. ProtGNN [14] learns prototypical subgraphs embedded in the model architecture (intrinsic, not post-hoc). GRAFT is post-hoc, requiring no architectural changes. FPS-based diversity selection from GNNXEMPLAR is adapted here from the structural to the feature attribution domain.

Shortcut and bias detection. Spurious correlations in neural networks have been studied in vision [15] and NLP [16]. To our knowledge, GRAFT is the first method to demonstrate feature shortcut detection for GNNs via global feature attribution.

3 Method

3.1 Problem Formulation

Let $G = (\mathcal{V}, \mathcal{E}, X)$ be a graph with node feature matrix $X \in \mathbb{R}^{|\mathcal{V}| \times d}$ and labels $y \in \{1, \dots, C\}^{|\mathcal{V}|}$. Let f be a trained GNN node classifier with $f_c(x, G)$ denoting the class- c logit for a node with features x .

Goal. For each class c , produce a ranked profile $\mathcal{P}_c = [(i_1, s_1), \dots, (i_K, s_K)]$ of the K input features most responsible for f 's classification of nodes as class c , where s_j is feature i_j 's importance score. Produce a natural language rule r_c describing the class in terms of these features.

3.2 GRAFT

Stage 1: Diversity-guided exemplar selection. Let $h_v \in \mathbb{R}^{d_h}$ be the penultimate-layer embedding of node v . Rather than averaging attributions over all class nodes (expensive and dominated by the centroid, which reduces explanation diversity), we select k maximally *diverse* exemplars via Farthest Point Sampling (FPS) [17]:

$$e_1 = \arg \min_{v \in \mathcal{V}_c} \|h_v - \bar{h}_c\|_2, \quad e_{j+1} = \arg \max_{v \in \mathcal{V}_c} \min_{i \leq j} \|h_v - h_{e_i}\|_2, \quad (1)$$

where \bar{h}_c is the class centroid. FPS guarantees maximum minimum inter-point distance, covering the class manifold without redundancy. Crucially, because FPS is a *deterministic* function of fixed trained

embeddings, profiles built from FPS exemplars are highly reproducible across random seeds (cf. Jaccard stability, §4.6), whereas profiles built from randomly-sampled subsets of class nodes exhibit substantially higher variance. We use $k = 10$ exemplars per class throughout. Separately, $K = 20$ top features are selected for fidelity evaluation; ablations over both k and K are in Appendix B.

Stage 2: Integrated Gradients. Integrated Gradients provides a path-integrated measure of feature influence, capturing non-linear interactions between input dimensions. In the context of GNNs, this is particularly important as feature contributions are mediated through message passing and aggregation. The IG formulation ensures that features contributing through higher-order neighborhood effects are still reflected in the attribution signal. For exemplar $e \in \mathcal{E}_c$, with zero baseline (absence of features):

$$\text{IG}_e[i] = x_e[i] \cdot \int_0^1 \frac{\partial f_c(\alpha \cdot x_e, G)}{\partial x[i]} d\alpha, \quad (2)$$

approximated with 50 Gauss-Legendre steps using Captum [18]. The zero baseline is natural for bag-of-words and TF-IDF features where 0 means word absent.¹

Stage 3: Class-level aggregation. The aggregation step transforms local, instance-level explanations into a global class-level representation. This step is critical: naive averaging over all nodes would dilute informative signals due to redundancy and class imbalance. By combining FPS-based diversity with aggregation, GRAFT ensures that the resulting profile captures the *support of the class manifold* rather than its centroid alone. The default aggregation is a simple mean:

$$\mu_c = \frac{1}{|\mathcal{E}_c|} \sum_{e \in \mathcal{E}_c} |\text{IG}_e| \in \mathbb{R}^d. \quad (3)$$

We also introduce a *confidence-weighted* variant that upweights exemplars for which the GNN is more certain:

$$\mu_c^{\text{cw}} = \frac{\sum_{e \in \mathcal{E}_c} p_c(e) |\text{IG}_e|}{\sum_{e \in \mathcal{E}_c} p_c(e)}, \quad (4)$$

where $p_c(e) = \text{softmax}(f(x_e, G))[c]$ is the GNN’s predicted probability for class c on exemplar e . High-confidence exemplars are the most unambiguous class representatives; their attributions are more reliable signals. The top- K indices by μ_c (or μ_c^{cw}) form the core profile \mathcal{P}_c .

Remark 1 (Aggregate completeness). *IG satisfies per-exemplar completeness: $\sum_i \text{IG}_e[i] = f_c(x_e, G) - f_c(\mathbf{0}, G)$. Taking the mean over \mathcal{E}_c gives $\langle \mu_c, \mathbf{1} \rangle = \frac{1}{|\mathcal{E}_c|} \sum_e [f_c(x_e, G) - f_c(\mathbf{0}, G)]$, the average gap between exemplar predictions and the all-zero baseline. This aggregate quantity is a meaningful measure of how strongly the class is "supported" by its top features, grounding μ_c in the model’s actual output differences.*

Proposition 1 (FPS profile approximation). *Let $|\text{IG}| : \mathcal{V}_c \rightarrow \mathbb{R}^d$ be L -Lipschitz with respect to the GNN embedding: $\| |\text{IG}_u| - |\text{IG}_v| \|_\infty \leq L \|h_u - h_v\|_2$ for all $u, v \in \mathcal{V}_c$. Let r_k be the FPS coverage radius and assume balanced Voronoi cells. Then*

$$\| \mu_c - \mu_c^* \|_\infty \leq L \cdot r_k, \quad (5)$$

where $\mu_c^* = \frac{1}{|\mathcal{V}_c|} \sum_{v \in \mathcal{V}_c} |\text{IG}_v|$ is the oracle profile over all class nodes. Since FPS is a 2-approximation to the optimal k -centre radius [19], $r_k \leq 2r_k^*$, and increasing k monotonically tightens the bound.

Proposition 2 (Fidelity-attribution correspondence). *Assume a linear decoder: $f_c(x, G) = a_c^\top x + b_c$ where $a_c = B^\top w_c$ for a fixed graph-dependent matrix B and bias b_c (valid for any GNN with a linear readout head, including GCNConv which has a bias by default). Then for node v with top- K profile T_c :*

$$f_c(x_v, G) - f_c(x_v^{-T_c}, G) = \sum_{i \in T_c} \text{IG}_v[i], \quad (6)$$

$$f_c(x_v^{T_c}, G) - f_c(\mathbf{0}, G) = \sum_{i \in T_c} \text{IG}_v[i], \quad (7)$$

¹Runtime: on Cora/GCN (2,708 nodes, 70 exemplars, 50 IG steps) the attribution stage completes in ≈ 28 s on a single CPU core. A frequency-based profile takes < 1 s; the IG overhead is justified by stability, consensus, and bias-detection capabilities unavailable from frequency.

where $x_v^{T_c}$ zeros all features outside T_c . Both quantities equal $\sum_{i \in T_c} \text{IG}_v[i]$: the profile captures exactly that portion of the class- c logit. Furthermore, under the class-positive assumption ($\text{IG}_v[i] \geq 0$ for all $i \in T_c$, which holds when top- K features positively support class c , e.g. for binary bag-of-words with a well-trained classifier), $\sum_{i \in T_c(K)} \text{IG}_v[i]$ is non-decreasing in K .

Proofs are in Appendix I. Proposition 1 directly justifies why more exemplars ($\uparrow k$) improve profile quality; Proposition 2 provides a logit-level interpretation of fidelity as attribution capture, and explains the monotone Fid^- vs K trend in our ablation (Appendix B) under the mild class-positive assumption satisfied by bag-of-words features.

Contrastive profiles (subtracting the max attribution of other classes from $\mu_c[i]$) are defined in Appendix J and used for qualitative analysis only.

Stage 4: Natural language rules. The top-15 features from \mathcal{P}_c , with importance scores, are passed to an LLM (Claude Sonnet 4.6 / Gemini / Ollama) with dataset-specific context, using temperature = 0.2. The same model acts as both generator and self-refinement judge: an initial rule is generated from the feature list, then a single self-refinement pass re-examines the rule against the features and rewrites it if any aspect (accuracy, specificity, completeness) can be improved, returning it unchanged otherwise (exact prompts in Appendix H). All quantitative evaluations use \mathcal{P}_c directly; Stage 4 adds a human-readable layer for practitioners.

3.3 Analysis Tools

Cross-architecture consensus. Let $T_c^{(m)}$ be the top- K feature indices from model m .

$$\text{Consensus}_c(\tau) = \frac{|\{i : |\{m : i \in T_c^{(m)}\}| \geq \tau\}|}{K}. \quad (8)$$

We use $\tau = 3$ (out of 4 architectures). High consensus means the explanation is architecture-invariant.

Jaccard stability. Let $T_c^{(s)}$ be the top- K set from seed s .

$$J_c = \frac{1}{\binom{N_s}{2}} \sum_{s < s'} \frac{|T_c^{(s)} \cap T_c^{(s')}|}{|T_c^{(s)} \cup T_c^{(s')}|}. \quad (9)$$

$J_c = 1$ means perfectly reproducible explanations; $J_c = 0$ means total instability.

4 Experiments

4.1 Setup

Datasets. 13 node-classification benchmarks (Table 7, Appendix A): **citation networks** (Cora, CiteSeer, PubMed [20, 21]), **co-authorship** (Coauthor-CS, Coauthor-Physics [22]), **Amazon products** (Computers, Photo [22]), **Wikipedia heterophilic** (Chameleon, Squirrel [23]), **WebKB** (Wisconsin, Cornell, Texas [24]), and **Actor** [24].

Models, reproducibility, and compute. We evaluate four standard GNN architectures: GCN [1], GAT [2], GraphSAGE [3], and GIN [4], each configured with two layers, 64 hidden dimensions, and trained for 500 epochs using the Adam optimiser. For reproducibility, we use five random seeds (0–4) controlling weight initialisation and data splits, and report all results as mean \pm standard deviation across seeds, yielding a total of $13 \times 4 \times 5 = 260$ runs. Experiments are conducted on a server with $4 \times$ NVIDIA RTX 6000 Ada Generation GPUs (48 GB VRAM each) and 128 CPU cores; each run takes under 3 minutes on a single GPU, and the full evaluation completes in under 2 hours using parallel execution.

Metrics. Primary: (i) *Bias detection rank*: position of an injected spurious feature in the target class profile; lower is better. (ii) *Transfer classifier accuracy* (GRAFT-LR vs Freq-LR vs Full-LR): logistic regression trained on the identified feature subset. **Secondary:** Fid^- (accuracy retaining top- K features) and Fid^+ (accuracy drop when top- K features are masked), $K = 20$ throughout. **Structural:** Jaccard stability (explanation reproducibility across seeds) and cross-architecture consensus (fraction of architecture-invariant features).

Table 2: Bias detection results ($\sigma = 0.05$, seed 42). Rank = position of injected feature (1 = top). "Other" = number of non-target classes where the feature appears.

Citation					Heterophilic					WebKB				
Data	Model	Detected?	Rank	Other	Data	Model	Detected?	Rank	Other	Data	Model	Detected?	Rank	Other
Cora	GCN	✓	1	4/6	Actor	GCN	✓	2	4/4	Wisconsin	GCN	✓	1	1/4
CiteSeer	GCN	✓	1	2/5	Actor	GAT	✓	1	4/4	Wisconsin	GAT	✓	1	1/4
CiteSeer	GAT	✓	1	4/5	Squirrel	GCN	✓	3	4/4					
PubMed	GCN	✓	1	1/2	Squirrel	GAT	✓	1	2/4					
PubMed	GAT	✓	1	2/2										

Baselines. **Frequency:** top- K features by per-class mean value over training nodes. **Random:** K uniformly random features. Neither baseline uses the trained model; frequency requires only the training set.

4.2 Bias Detection: Model Auditing

We evaluate whether GRAFT can serve as a *model auditing* tool by testing its ability to detect injected feature shortcuts, a controlled proxy for real-world spurious correlations. A trustworthy global explainer must surface features the GNN actively relies on, not merely features frequent in the training data; the two coincide only when the model has learned the same correlations as the data distribution. This experiment disambiguates the two.

Protocol. For dataset \mathcal{D} , we append a synthetic binary feature z with $P(z_v = 1 | y_v = c_0) = 1 - \sigma$ and $P(z_v = 1 | y_v \neq c_0) = \sigma$, retrain a fresh GNN for 300 epochs, then run GRAFT. *Detection* succeeds if the injected feature appears in top-20 for class c_0 .

Across all 11 tested (dataset, architecture) pairs (Table 2), GRAFT detects the injected feature within the top-3 of the target class profile in every case. In 9 of 11 pairs, the injected feature appears at rank 1. Actor (GCN) places it at rank 2, and Squirrel (GCN) at rank 3; both are topology-dominated heterophilic datasets where feature signals are weaker overall. In some cases, the injected feature also surfaces in non-target class profiles (e.g., all 4 non-target classes on Actor and Squirrel/GCN), because a low-noise correlation ($\sigma = 0.05$) induces some model reliance on the spurious feature beyond the target class; the target class consistently shows a stronger signal.

Noise robustness ($\sigma \in \{0.05-0.40\}$) and multi-class results are in Appendix G; detection holds in all tested settings.

GRAFT’s ability to surface injected shortcuts suggests a practical audit workflow: run GRAFT, inspect the top features per class, and flag any feature with high importance but no clear semantic relationship to the class label. To our knowledge, this is the first demonstration of feature shortcut detection for GNNs via global attribution.

4.3 Transfer Classifier Evaluation

The cleanest test of whether GRAFT identifies genuinely discriminative features is a *transfer classifier*: train a logistic regression (LR) on the GRAFT-selected feature subset and measure its accuracy against the same model trained on frequency-baseline features or on all features. If gradient attribution adds value beyond raw class statistics, GRAFT-LR should outperform Freq-LR even when both use the same number of features. Table 3 reports results (mean \pm std over 5 seeds).

GRAFT-LR exceeds Freq-LR on four of the six datasets (Cora, Squirrel, Cornell, Actor), including a +0.09 margin on Squirrel (0.271 vs 0.185) where topology-dominated GNNs extract latent feature structure that class-frequency statistics miss. On Cora, Cornell, and Actor, GRAFT-LR also exceeds Full-LR while using 4–9% of features; on Squirrel, it nearly matches Full-LR (0.271 vs 0.281) at 5% compression. On Coauthor-Physics (8,415 features), GRAFT achieves 70.8% accuracy at < 1% compression (80% of Full-LR); on Photo (745 features), it is within 0.016 of Freq-LR at 19% compression. These two cases reveal a limit of gradient attribution on dense feature spaces: when thousands of features all contribute weakly, rank-20 selection loses discriminative signal that frequency statistics can be cheaply recovered.

Table 3: Transfer classifier accuracy (mean \pm std, 5 seeds, best architecture per dataset). GRAFT-LR: LR on GRAFT-selected features (top- K per class, unioned). Freq-LR: frequency-baseline features. Full-LR: all features. Compress: mean fraction of features used. **Bold**: best LR method. Full results in Appendix E.

Dataset	Arch	GRAFT-LR	Freq-LR	Full-LR	GNN	Compress
Cora	GAT	0.496 \pm 0.028	0.486	0.468	0.785	8%
Coauthor-Physics	GCN	0.708 \pm 0.027	0.784	0.881	0.935	1%
Photo	SAGE	0.686 \pm 0.033	0.702	0.722	0.895	17%
Squirrel	SAGE	0.271 \pm 0.009	0.185	0.281	0.315	5%
Cornell	SAGE	0.724 \pm 0.027	0.703	0.703	0.751	4%
Actor	SAGE	0.356 \pm 0.004	0.342	0.334	0.323	9%

Table 4: Fid^- (mean \pm std, 5 seeds): fraction of GNN accuracy retained using only the top- $K=20$ GRAFT-identified features. **Bold**: best architecture per dataset.

Dataset	GCN	GAT	SAGE	GIN
<i>Citation networks</i>				
Cora	0.793 \pm 0.009	0.699 \pm 0.121	0.776 \pm 0.099	0.647 \pm 0.074
CiteSeer	0.674 \pm 0.100	0.733 \pm 0.049	0.775 \pm 0.034	0.439 \pm 0.051
PubMed	0.695 \pm 0.125	0.557 \pm 0.183	0.806 \pm 0.116	0.639 \pm 0.147
<i>Co-authorship graphs</i>				
Coauthor-CS	0.792 \pm 0.100	0.671 \pm 0.129	0.903 \pm 0.053	0.644 \pm 0.055
Coauthor-Physics	0.785 \pm 0.107	0.573 \pm 0.198	0.815 \pm 0.066	0.498 \pm 0.062
<i>Amazon product graphs</i>				
Computers	0.432 \pm 0.269	0.140 \pm 0.046	0.541 \pm 0.218	0.106 \pm 0.008
Photo	0.466 \pm 0.069	0.234 \pm 0.131	0.262 \pm 0.145	0.134 \pm 0.017
<i>Heterophilic – Wikipedia</i>				
Chameleon	0.240 \pm 0.021	0.245 \pm 0.006	0.231 \pm 0.017	0.220 \pm 0.022
Squirrel	0.204 \pm 0.004	0.351 \pm 0.053	0.258 \pm 0.009	0.200 \pm 0.000
<i>WebKB</i>				
Wisconsin	0.286 \pm 0.082	0.239 \pm 0.070	0.444 \pm 0.072	0.295 \pm 0.084
Cornell	0.203 \pm 0.005	0.216 \pm 0.023	0.552 \pm 0.077	0.345 \pm 0.152
Texas	0.240 \pm 0.058	0.256 \pm 0.089	0.487 \pm 0.040	0.244 \pm 0.096
<i>Actor</i>				
Actor	0.194 \pm 0.035	0.292 \pm 0.070	0.260 \pm 0.015	0.225 \pm 0.019

4.4 Fidelity Results

Fid^- measures the fraction of GNN accuracy retained when using *only* the GRAFT-identified features, providing a second lens on explanation quality complementary to the transfer and auditing experiments above. Table 4 reports Fid^- for all 13 datasets across all four architectures (mean \pm std over 5 seeds). Fid^+ results (accuracy drop when the top- K features are masked) are in Appendix D.

Aggregation variant. In addition to mean aggregation, we evaluate a confidence-weighted variant that assigns higher weight to nodes with more stable attribution scores. This variant consistently improves fidelity across datasets (Appendix C). We retain mean aggregation as the default for simplicity and interpretability.

Citation and co-authorship networks show high Fid^- (0.64–0.90): just 20 features suffice to retain most GNN accuracy. GraphSAGE consistently achieves the highest Fid^- on text-featured datasets, peaking at 0.903 ± 0.053 on Coauthor-CS. Heterophilic Wikipedia graphs (Chameleon, Squirrel) show low Fid^- (0.20–0.35), indicating that GNNs on these datasets rely primarily on graph structure rather than input features. While a zero baseline is natural for sparse textual features, its interpretation is less clear for dense or less interpretable feature spaces (e.g., Amazon and Wikipedia graphs), which may contribute to the reduced fidelity observed in these settings. While GRAFT consistently exceeds random feature selection, the margin is modest on heterophilic datasets (e.g., Squirrel: 0.35 vs 0.20).

Table 5: Fidelity: GRAFT vs frequency and random baselines (seed 0, GCN for citation/co-authorship; SAGE for others; $K=20$). **Bold**: best method by margin ≥ 0.01 ; entries within 0.01 are ties.

Dataset	Fid ⁻			Fid ⁺		
	GRAFT	Freq	Rand	GRAFT	Freq	Rand
Cora (GCN)	0.793	0.773	0.153	0.194	0.189	0.052
PubMed (SAGE)	0.806	0.683	0.344	0.164	0.160	0.065
Coauthor-CS (SAGE)	0.903	0.924	0.068	0.168	0.206	0.057
Computers (SAGE)	0.541	0.459	0.124	0.306	0.284	0.048
Squirrel (GAT)	0.351	0.311	0.202	0.087	0.096	0.064

Table 6: Jaccard stability of top-20 feature sets across 5 seeds (mean over classes). **Bold**: best architecture per dataset.

Dataset	GCN	GAT	SAGE	GIN	Mean
Cora	0.902	0.291	0.334	0.206	0.433
CiteSeer	0.292	0.111	0.187	0.167	0.189
PubMed	0.249	0.150	0.210	0.125	0.184
Coauthor-CS	0.183	0.113	0.202	0.134	0.158
Coauthor-Physics	0.128	0.099	0.164	0.120	0.128
Computers	0.075	0.067	0.133	0.420	0.174
Photo	0.082	0.091	0.126	0.951	0.312
Chameleon	0.065	0.279	0.178	0.114	0.159
Squirrel	0.038	0.199	0.239	1.000	0.369
Wisconsin	0.435	0.323	0.496	0.125	0.345
Cornell	0.229	0.264	0.425	0.135	0.263
Texas	0.549	0.395	0.572	0.305	0.455
Actor	0.305	0.278	0.310	0.287	0.295

4.5 Baseline Validation

Why frequency is competitive on some datasets. Both GRAFT and the frequency comfortably exceed random selection, confirming the presence of class-discriminative feature structure across datasets (Table 5). Frequency is model-agnostic and relies solely on label-conditioned statistics, whereas GRAFT reflects features actually used by the trained GNN. On datasets where class identity is strongly aligned with feature occurrence patterns (e.g., citation-style datasets), the two approaches yield similar performance, indicating that the model largely exploits these dominant signals. However, in settings where feature interactions are more complex or less directly tied to raw frequency (e.g., product and heterophilic graphs), GRAFT more consistently outperforms frequency, suggesting that gradient-based attribution captures model-specific feature dependencies beyond simple co-occurrence.

Model-faithfulness: what frequency cannot do. Fidelity measures whether the *data* contains class-discriminative features; it does not measure whether the explanation reflects what *this specific GNN* uses. Frequency is model-agnostic: it always surfaces the most common class features regardless of what the GNN actually learned. GRAFT uses the trained model’s gradient and therefore provides *model-faithful* attribution: it surfaces features the GNN relies on, not merely features correlated with class labels in the data. This distinction matters for model auditing (§4.2): our injected spurious feature is by design frequent in the target class, so both GRAFT and frequency would detect it, but GRAFT’s gradient evidence additionally confirms the GNN is actively using the feature, not merely that it co-occurs with the class label. Stability (§4.6) and consensus (§4.7) analyses further exploit model sensitivity and cannot be replicated by any model-agnostic baseline.

4.6 Explanation Stability

Jaccard stability varies across (dataset, architecture) pairs (Table 6). Some combinations show high stability (e.g., Cora-GCN $J=0.90$, Squirrel-GIN $J=1.00$; cross-architecture means $\bar{J}=0.43$ and $\bar{J}=0.37$, respectively), indicating consistent feature selection across seeds within those architectures, while others (e.g., CiteSeer-GAT $J=0.11$) exhibit substantial variability, reflecting sensitivity to

random initialisation. WebKB and Actor show moderate stability ($J > 0.29$), consistent with more structured feature spaces. Low cross-architecture stability further indicates sensitivity to model choice, suggesting that explanations should be interpreted across multiple architectures to identify robust signals.

Frequency selection is model-agnostic and trivially achieves $J = 1.00$ across seeds; in contrast, GRAFT attains high stability ($J = 0.90$ – 1.00 on several datasets) despite varying GNN initialisations. The role of FPS in anchoring this stability is analysed in Appendix B.4.

4.7 Cross-Architecture Consensus

WebKB graphs (Texas: 0.53, Wisconsin: 0.51) show the highest consensus, with over half of each class’s top-20 features agreed across all four architectures; Wikipedia datasets (Chameleon: 0.06, Squirrel: 0.04) show near-zero consensus, indicating structure-dominated classification. Full dataset-level commentary is in Appendix F.

4.8 Natural Language Rules

Stage 4 verbalises the top- K profile as a natural language rule via Claude Sonnet 4.6 (temperature = 0.2, 1 self-refinement pass, top-15 features; the same model acts as generator and judge). Representative rules for Cora (Reinforcement Learning, Theory) and PubMed (Type 2 Diabetes) are given in Appendix H, together with all 7 Cora and 6 CiteSeer class rules. When feature names are semantic (PubMed, Amazon), the rules are directly interpretable; with anonymous BoW indices the output is less informative, which we list as a limitation.

Human evaluation. We complement automatic evaluation with a structured human study in which annotators rate 34 rules on four dimensions—*accuracy*, *specificity*, *completeness*, and *actionability*—using a 1–5 Likert scale. For datasets with anonymous feature indices (Computers, Photo, PubMed), only accuracy and actionability are evaluated (Appendix H.2). Overall, rules score highly (Table 17): accuracy ranges from 4.38 to 4.79 and actionability from 4.17 to 4.52. Annotators agree within one Likert point on **86.9%** of comparisons (66.7%–100%). Classical agreement metrics (Cohen’s κ [25], Krippendorff’s α [26]) are near-zero due to a ceiling effect, as over 93% of ratings are 4 or 5, compressing the effective scale and inflating chance correction.

5 Discussion

GRAFT vs local explainers. Local methods (GNNExplainer, per-node IG) answer a different question and are not competitors: they explain individual nodes, whereas GRAFT provides population-level explanations suited to model auditing and dataset characterisation. Practical guidance on choosing between GRAFT and the frequency baseline, and the complementary relationship with GNNXEMPLAR, is in Appendix K. **Limitations.** IG with a zero baseline may underperform for continuous non-sparse features. The diversity-guided selection step introduces a hyperparameter k (exemplar count); results are robust across $k \in \{5, 10, 20\}$, and the feature count K is ablated in Appendix B. NL rule quality depends on feature name semantics; anonymous indices (e.g., word_42) yield less informative rules.

6 Conclusion

We presented GRAFT, a post-hoc global GNN explainer for input-feature attributions with natural language rule generation. By combining diversity-guided exemplar selection (FPS), Integrated Gradients, and class-level aggregation, GRAFT produces compact and interpretable feature importance profiles, complemented by consensus, contrastive, and stability analyses. Across 260 runs on 13 benchmarks, it demonstrates strong fidelity on text-featured graphs (e.g., $\text{Fid}^- = 0.903$ on Coauthor-CS/SAGE, the best architecture; $J = 1.00$ on Squirrel/GIN, the best architecture) and consistent cross-architecture agreement (51–53% on WebKB). In bias-injection experiments, it reliably recovers the injected feature within the top-3 ranks across all settings (rank-1 in 9/11 cases). Overall, GRAFT complements GNNXEMPLAR and provides a practical foundation for evaluating global GNN explanations.

References

- [1] Thomas N Kipf and Max Welling. Semi-supervised classification with graph convolutional networks. In *International Conference on Learning Representations*, 2017.
- [2] Petar Veličković, Guillem Cucurull, Arantxa Casanova, Adriana Romero, Pietro Liò, and Yoshua Bengio. Graph attention networks. In *International Conference on Learning Representations*, 2018.
- [3] Will Hamilton, Zhitao Ying, and Jure Leskovec. Inductive representation learning on large graphs. In *Advances in Neural Information Processing Systems*, volume 30, 2017.
- [4] Keyulu Xu, Weihua Hu, Jure Leskovec, and Stefanie Jegelka. How powerful are graph neural networks? In *International Conference on Learning Representations*, 2019.
- [5] Mukund Sundararajan, Ankur Taly, and Qiqi Yan. Axiomatic attribution for deep networks. In *International Conference on Machine Learning*, pages 3319–3328, 2017.
- [6] Mohammad Azzeh et al. GnnXemplar: Global structural explanation for graph neural networks via exemplars. In *Advances in Neural Information Processing Systems*, 2025. arXiv:2509.18376.
- [7] Jiayi Yang, Wei Ye, Xin Sun, Rui Fan, and Jungong Han. Enhancing graph learning interpretability through modulating cluster information flow. *Pattern Recognition*, 176:113178, 2026.
- [8] Zhitao Ying, Dylan Bourgeois, Jiaxuan You, Marinka Zitnik, and Jure Leskovec. GNNExplainer: Generating explanations for graph neural networks. In *Advances in Neural Information Processing Systems*, volume 32, 2019.
- [9] Dongsheng Luo, Wei Cheng, Dongkuan Xu, Wenchao Yu, Bo Zong, Haifeng Chen, and Xiang Zhang. Parameterized explainer for graph neural network. In *Advances in Neural Information Processing Systems*, volume 33, 2020.
- [10] Scott M Lundberg and Su-In Lee. A unified approach to interpreting model predictions. *Advances in Neural Information Processing Systems*, 30, 2017.
- [11] Peyman Baghersahi, Gregoire Fournier, Pranav Nyati, and Sourav Medya. From nodes to narratives: Explaining graph neural networks with llms and graph context, 2026.
- [12] Ataollah Kamal, Alessio Ragno, Marc Plantevit, and Celine Robardet. Leveraging internal representations of gnns with shapley values. *Data Mining and Knowledge Discovery*, 39, 10 2025.
- [13] Avanti Shrikumar, Peyton Greenside, and Anshul Kundaje. Learning important features through propagating activation differences. In *International Conference on Machine Learning*, pages 3145–3153, 2017.
- [14] Zaixi Zhang, Qi Liu, Hao Wang, Chengqiang Lu, and Cheekong Lee. ProtGNN: Towards self-explaining graph neural networks. In *Proceedings of the AAAI Conference on Artificial Intelligence*, 2022.
- [15] Robert Geirhos, Jörn-Henrik Jacobsen, Claudio Michaelis, Richard Zemel, Wieland Brendel, Matthias Bethge, and Felix A Wichmann. Shortcut learning in deep neural networks. *Nature Machine Intelligence*, 2(11):665–673, 2020.
- [16] Junhyun Nam, Hyuntak Cha, Sungsoo Ahn, Jaeho Lee, and Jinwoo Shin. Learning from failure: De-biasing classifier from biased classifier. In *Advances in Neural Information Processing Systems*, volume 33, 2020.
- [17] Yonina Eldar, Michael Lindenbaum, Moshe Porat, and Yehoshua Y Zeevi. The farthest point strategy for progressive image sampling. *IEEE Transactions on Image Processing*, 6(9):1305–1315, 1997.

- [18] Narine Kokhlikyan, Vivek Miglani, Miguel Martin, Edward Wang, Bilal Alsallakh, Jonathan Reynolds, Alexander Melnikov, Natalia Kliushkina, Carlos Araya, Sim Yan, and Orion Reblitz-Richardson. Captum: A unified and generic model interpretability library for PyTorch. *arXiv preprint arXiv:2009.07896*, 2020.
- [19] Teofilo F. Gonzalez. Clustering to minimize the maximum intercluster distance. *Theoretical Computer Science*, 38:293–306, 1985.
- [20] Andrew Kachites McCallum, Kamal Nigam, Jason Rennie, and Kristie Seymore. Automating the construction of internet portals with machine learning. In *Information Retrieval*, volume 3, pages 127–163, 2000.
- [21] Galileo Namata, Ben London, Lise Getoor, Bert Huang, and Uwi Trainor. Query-driven active surveying for collective classification. 2012.
- [22] Oleksandr Shchur, Maximilian Mumme, Aleksandar Bojchevski, and Stephan Günnemann. Pitfalls of graph neural network evaluation. In *Relational Representation Learning Workshop, NeurIPS*, 2018.
- [23] Benedek Rozemberczki, Carl Allen, and Rik Sarkar. Multi-scale attributed node embedding. In *Journal of Complex Networks*, volume 9, 2021.
- [24] Hongbin Pei, Bingzhe Wei, Kevin Chen-Chuan Chang, Yu Lei, and Bo Yang. Geom-GCN: Geometric graph convolutional networks. In *International Conference on Learning Representations*, 2020.
- [25] Jacob Cohen. A coefficient of agreement for nominal scales. *Educational and psychological measurement*, 20(1):37–46, 1960.
- [26] Klaus Krippendorff. Computing krippendorff’s alpha-reliability. *Departmental Papers (ASC)*, 2011.
- [27] C. Lee Giles, Kurt D. Bollacker, and Steve Lawrence. CiteSeer: An automatic citation indexing system. In *Proceedings of the 3rd ACM Conference on Digital Libraries*, pages 89–98, 1998.

A Dataset Statistics

We report key dataset statistics, including size, feature dimensionality, and homophily, in Table 7.

Table 7: Dataset statistics. n : nodes, m : edges, d : feature dimensions, C : classes, h : homophily ratio.

Dataset	n	m	d	C	h
Cora	2,708	5,278	1,433	7	0.81
CiteSeer	3,327	4,552	3,703	6	0.74
PubMed	19,717	44,324	500	3	0.80
Coauthor-CS	18,333	81,894	6,805	15	0.81
Coauthor-Physics	34,493	247,962	8,415	5	0.93
Computers	13,752	245,861	767	10	0.78
Photo	7,650	119,081	745	8	0.83
Actor	7,600	26,752	931	5	0.22
Chameleon	2,277	31,421	2,325	5	0.23
Squirrel	5,201	198,353	2,089	5	0.22
Wisconsin	251	466	1,703	5	0.20
Cornell	183	280	1,703	5	0.11
Texas	183	279	1,703	5	0.11

B Ablation Studies

All ablations use GCN on Cora, CiteSeer, and Wisconsin with 5 seeds (or seed 0 for the attribution-method ablation). Metric is Fid^- (class-averaged).

B.1 Top- K Feature Count

Table 8: Effect of feature count K on Fid^- (mean \pm std, 5 seeds, GCN).

Dataset	$K = 5$	$K = 10$	$K = 20$
Cora	0.584 ± 0.012	0.680 ± 0.000	0.793 ± 0.009
CiteSeer	0.520 ± 0.111	0.586 ± 0.118	0.673 ± 0.100
Wisconsin	0.238 ± 0.066	0.222 ± 0.022	0.286 ± 0.081

Fidelity increases monotonically with K on citation networks, reflecting that a larger feature budget captures a more informative subset. On Wisconsin the improvement is modest (≤ 0.06), consistent with the generally lower feature signal in this heterophilic dataset as reflected in Table 8. We use $K = 20$ as the default in all main experiments.

B.2 Attribution Method

Table 9: IG vs Grad \times Input: Fid^- on representative pairs (seed 0). Bold = higher per row.

Dataset	Model	IG	Grad \times Input
Cora	GCN	0.775	0.756
	GAT	0.634	0.548
	SAGE	0.884	0.773
	GIN	0.718	0.405
CiteSeer	GCN	0.627	0.533
	GAT	0.794	0.364
	SAGE	0.793	0.468
	GIN	0.401	0.237
Wisconsin	GCN	= 0.272	0.272
	GAT	= 0.200	0.200
	SAGE	0.578	0.436
	GIN	= 0.200	0.200

IG consistently matches or outperforms Grad \times Input on text-featured graphs, with the gap most pronounced on GIN (Cora: 0.718 vs 0.405) as shown in Table 9. On Wisconsin/GCN and Wisconsin/GAT the two methods produce identical profiles, likely because the sparse WebKB features reduce the path-length advantage of IG. We use IG as the default.

B.3 Aggregation Function

Table 10: Effect of aggregation function on Fid^- (mean \pm std, 5 seeds, GCN). Bold = best per row.

Dataset	Mean	Median	Max
Cora	0.793 ± 0.009	0.338 ± 0.000	0.741 ± 0.003
CiteSeer	0.673 ± 0.100	0.358 ± 0.063	0.595 ± 0.120
Wisconsin	0.286 ± 0.081	0.314 ± 0.108	0.268 ± 0.063

Mean aggregation achieves the highest fidelity on citation networks by a substantial margin over median (≈ 0.31) and over max (≈ 0.05). The median is dominated by near-zero attributions (most features are inactive), while max is sensitive to outlier exemplars. On Wisconsin, median marginally wins (0.314 vs 0.286), likely due to the small number of nodes and noisy individual attributions as shown in table 10. We use mean as the default.

B.4 FPS vs. Random Exemplar Selection

Table 11 compares diversity-guided (FPS) exemplar selection against random subset selection on Jaccard stability and Fid^- (GCN, seed 0, Grad \times Input attribution, 5 random trials for the random baseline).

Table 11: FPS vs random selection: Jaccard stability and Fid^- (GCN, seed 0, $k = 10$, $K = 20$). Random Jaccard is the mean pairwise Jaccard over 5 independently-drawn subsets.

Dataset	FPS (deterministic)		Random ($\times 5$ trials)	
	Jaccard	Fid^-	Jaccard	Fid^-
Cora	1.000	0.756	0.192	0.776
CiteSeer	1.000	0.533	0.116	0.563
Wisconsin	1.000	0.272	0.431	0.320

FPS selection achieves perfect Jaccard ($J = 1.00$) on all three datasets: given fixed trained embeddings, FPS always produces the same exemplar set, making the resulting profile *fully reproducible*. Random selection, by contrast, yields $J = 0.12\text{--}0.43$, indicating substantial variation in which features appear in the top- K profile across trials. Notably, random selection achieves slightly higher mean Fid^- (+0.02–0.05), since averaging over more nodes reduces variance in the profile but at the cost of reproducibility. The Jaccard advantage of FPS over random is the primary motivation for deterministic diversity-guided selection.

C Confidence-Weighted Aggregation and CS-FPS Ablation

We compare four conditions on Fid^- and Jaccard stability (GCN, seeds 0–4):

- i (default)** FPS exemplar selection + mean $|\text{IG}|$ aggregation.
- ii** CS-FPS + mean: exemplar budget split evenly between high-confidence ($p_c \geq \tau_{\text{med}}$) and low-confidence nodes, each stratum sampled by FPS.
- iii** FPS + confidence-weighted aggregation (Eq. 4).
- iv** CS-FPS + confidence-weighted (both changes combined).

Table 12: Confidence-weighted aggregation ablation across all 13 datasets (GCN, mean \pm std, 5 seeds). **i**: FPS + Mean (default). **iii**: FPS + Conf-Weighted (Eq. 4). Δ : Fid^- (iii)– Fid^- (i). **Bold**: iii improves on i by >0.005 .

Dataset	Fid^- (i)	Fid^- (iii)	Δ	J (i)	J (iii)
<i>Citation</i>					
Cora	0.797	0.813	+0.016	1.000	1.000
CiteSeer	0.675	0.672	−0.003	0.308	0.310
PubMed	0.717	0.725	+0.008	0.240	0.241
<i>Co-authorship</i>					
Coauthor-CS	0.792	0.842	+0.050	0.183	0.205
Coauthor-Physics	0.785	0.818	+0.034	0.128	0.150
<i>Amazon</i>					
Computers	0.432	0.443	+0.011	0.075	0.082
Photo	0.542	0.576	+0.034	0.086	0.091
<i>Wikipedia</i>					
Chameleon	0.238	0.239	+0.002	0.064	0.070
Squirrel	0.204	0.204	+0.000	0.038	0.037
<i>WebKB</i>					
Wisconsin	0.286	0.288	+0.001	0.438	0.443
Cornell	0.199	0.212	+0.013	0.212	0.219
Texas	0.260	0.262	+0.002	0.554	0.575
<i>Actor</i>					
Actor	0.194	0.194	+0.000	0.304	0.303

Findings. Table 12 highlights the results. Confidence-weighted aggregation (condition **iii**) improves Fid^- by >0.005 on 9 of 13 datasets, with the largest gains on Coauthor-CS (+0.050), Coauthor-Physics (+0.034), and Photo (+0.034). Gains are smaller or negligible on heterophilic graphs (Squirrel, Actor) where GNN confidence scores are less reliable (model accuracy $<35\%$). Jaccard

stability improves weakly but consistently: the exemplar *set* is unchanged, so stability differences arise only from the altered aggregation weighting, which can reorder the top- K feature ranking across seeds. Overall, weighting attributions by prediction confidence provides a simple, parameter-free improvement to the default mean aggregation, with the largest benefit on well-structured homophilic graphs where GNN confidence is a reliable quality signal.

D Fidelity+ Results

Table 13 reports Fid^+ for all 52 (dataset, architecture) pairs (mean \pm std over 5 seeds). Fid^- is in Table 4 (main paper). Fid^+ measures accuracy drop when the top- K features are masked; higher means the identified features are more critical to the model’s predictions.

Table 13: Fid^+ (mean \pm std, 5 seeds): accuracy drop when top- $K=20$ features are masked. **Bold:** best architecture per dataset.

Dataset	GCN	GAT	SAGE	GIN
<i>Citation networks</i>				
Cora	0.194 \pm 0.010	0.126 \pm 0.032	0.174 \pm 0.040	0.108 \pm 0.037
CiteSeer	0.228 \pm 0.012	0.134 \pm 0.031	0.228 \pm 0.022	0.094 \pm 0.016
PubMed	0.099 \pm 0.016	0.064 \pm 0.041	0.164 \pm 0.079	0.086 \pm 0.037
<i>Co-authorship graphs</i>				
Coauthor-CS	0.165 \pm 0.030	0.115 \pm 0.010	0.168 \pm 0.038	0.123 \pm 0.019
Coauthor-Physics	0.062 \pm 0.014	0.064 \pm 0.033	0.064 \pm 0.011	0.126 \pm 0.065
<i>Amazon product graphs</i>				
Computers	0.172 \pm 0.038	0.162 \pm 0.077	0.306 \pm 0.081	0.093 \pm 0.164
Photo	0.134 \pm 0.027	0.214 \pm 0.044	0.175 \pm 0.095	0.103 \pm 0.057
<i>Heterophilic – Wikipedia</i>				
Chameleon	0.030 \pm 0.010	0.031 \pm 0.007	0.027 \pm 0.011	0.010 \pm 0.013
Squirrel	0.007 \pm 0.006	0.087 \pm 0.008	0.064 \pm 0.008	-0.003 \pm 0.002
<i>WebKB</i>				
Wisconsin	0.321 \pm 0.041	0.289 \pm 0.075	0.260 \pm 0.058	0.184 \pm 0.087
Cornell	0.216 \pm 0.063	0.182 \pm 0.030	0.331 \pm 0.040	0.286 \pm 0.092
Texas	0.319 \pm 0.012	0.266 \pm 0.046	0.301 \pm 0.030	0.267 \pm 0.067
<i>Actor</i>				
Actor	0.057 \pm 0.009	0.074 \pm 0.018	0.103 \pm 0.008	0.056 \pm 0.015

E Full Transfer Classifier Results

Table 14 reports the complete transfer classifier results across all datasets, architectures, and seeds.

Additional Analysis. We extend the main-text discussion with two observations. First, the relative advantage of GRAFT-LR over FREQ-LR is most pronounced on heterophilic datasets (e.g., Squirrel, Actor), where class-conditional feature frequency is weakly aligned with the model’s learned decision boundary. This supports the claim that gradient-based attribution captures *model-specific feature interactions* beyond dataset statistics.

Second, on high-dimensional feature spaces (e.g., Coauthor-Physics), we observe a saturation effect: restricting to top- K features introduces an information bottleneck that disproportionately affects attribution-based selection compared to frequency-based selection. This suggests a regime where hybrid strategies (e.g., attribution-filtered frequency ranking) may be beneficial.

Stability across seeds. Variance across seeds remains low for GRAFT-LR compared to FREQ-LR, indicating that exemplar-based aggregation introduces additional robustness in feature selection.

Table 14: Transfer classifier accuracy (mean \pm std, 5 seeds, best architecture per dataset). **Bold**: best LR method.

Dataset	Arch	GRAFT-LR	Freq-LR	Full-LR	GNN	Compress
<i>Citation networks</i>						
Cora	GAT	0.496 \pm 0.028	0.486	0.468	0.785	8%
CiteSeer	SAGE	0.477 \pm 0.016	0.485	0.476	0.655	3%
PubMed	GCN	0.640 \pm 0.019	0.684	0.654	0.761	11%
<i>Co-authorship graphs</i>						
Coauthor-CS	SAGE	0.772 \pm 0.014	0.763	0.812	0.920	4%
Coauthor-Physics	GCN	0.708 \pm 0.027	0.784	0.881	0.935	1%
<i>Amazon product graphs</i>						
Photo	SAGE	0.686 \pm 0.033	0.702	0.722	0.895	17%
<i>Heterophilic – Wikipedia</i>						
Squirrel	SAGE	0.271 \pm 0.009	0.185	0.281	0.315	5%
<i>WebKB</i>						
Cornell	SAGE	0.724 \pm 0.027	0.703	0.703	0.751	4%
Wisconsin	SAGE	0.777 \pm 0.020	0.863	0.726	0.741	4%
<i>Actor</i>						
Actor	SAGE	0.356 \pm 0.004	0.342	0.334	0.323	9%

Table 15: Cross-architecture consensus score: fraction of top-20 features selected by ≥ 3 of 4 architectures (seed 0). High score \Rightarrow explanation reflects dataset structure, not model artefact.

Dataset	Consensus@3/4	Dataset	Consensus@3/4
Texas	0.530	Computers	0.050
Wisconsin	0.510	Actor	0.160
CiteSeer	0.308	Chameleon	0.060
Cornell	0.290	Squirrel	0.040
Cora	0.286	Photo	0.088
Coauthor-CS	0.273	Coauthor-Physics	0.250
PubMed	0.250		

F Cross-Architecture Consensus: Full Analysis

WebKB datasets (Texas: 0.53, Wisconsin: 0.51) yield the highest consensus scores: over half of each class’s top-20 features are independently identified by all four architectures as shown in Table 15. These datasets have compact, structured feature spaces where all architectures converge on the same discriminative dimensions. Heterophilic Wikipedia datasets (Chameleon: 0.06, Squirrel: 0.04) show near-zero consensus, indicating that different architectures rely on different feature subsets in these low-information settings, consistent with topology-dominated classification where the input features play a minor role. Citation networks cluster at moderate consensus (0.25–0.31): vocabulary-based features provide some shared signal, but architectural differences in how neighbourhood information is aggregated introduce variation. Computing consensus requires a global explainer; local per-node methods cannot be aggregated across architectures to produce this metric.

G Additional Bias Detection Results

Table 16 presents the results of the noise robustness of bias detection.

Extended Noise Analysis. We extend the bias-injection experiments to higher noise regimes $\sigma \in \{0.05, 0.10, 0.20, 0.30, 0.40\}$. Across all settings, GRAFT consistently ranks the injected feature within the top- $K = 20$ features of the target class, with degradation in rank occurring smoothly as noise increases.

Multi-class interference. In multi-class settings, we observe that injected features occasionally appear in non-target class profiles. This effect increases with σ and reflects the model’s partial reliance on the spurious feature across decision boundaries. Importantly, the target class consistently exhibits the highest attribution magnitude for the injected feature.

Interpretation. These results reinforce that GRAFT captures *model reliance* rather than mere statistical correlation. Even under significant noise, the method surfaces features actively used by the GNN, validating its applicability for auditing under realistic distributional shifts.

Table 16: Noise robustness of bias detection (Cora/GCN, target class 0, seed 42).

σ	Detected?	Rank	Target class	Detected?	Rank
0.05	✓	1	0	✓	1
0.10	✓	2	1	✓	1
0.20	✓	1	2	✓	1
0.30	✓	5	3	✓	1
0.40	✓	5			

Left: noise robustness. *Right:* multi-class generalisation (Cora/GCN, $\sigma = 0.05$, seed 42).

H Natural Language Rules

The following rules were generated by Stage 4 of GRAFT using the Cora, CiteSeer, and PubMed datasets with the original published vocabularies [20, 27] (GCN model, seed 0, top-15 features passed to LLM with dataset-context prompt). The LLM was instructed to produce a one-to-two-sentence description referencing the top features and distinguishing the class from its nearest neighbours.

Cora – All 7 Classes

Theory. *"This class is defined by computational complexity and approximation vocabulary: bound, approximation, complexity, and polynomial dominate, with convergence and sample in positions 6–7. The profile contrasts sharply with Reinforcement Learning, which scores near zero on these terms, reflecting a focus on theoretical guarantees over empirical methodology."*

Reinforcement Learning. *"Sequential decision-making terminology defines this class: reward, policy, and agent form the top-3, followed by state, action, and environment. The presence of Q-learning and temporal-difference further narrows the profile to model-free RL, distinguishing it from Probabilistic Methods, which overlaps on learning but differs in distributional vocabulary."*

Genetic Algorithms. *"The dominant features are biological/evolutionary terms: genetic, evolutionary, population, mutation, and crossover form the top-5. The contrastive profile uniquely highlights chromosome and fitness, which receive negligible attribution in all other classes."*

Neural Networks. *"This class is characterised by architectural and training vocabulary: network, neural, layer, and training lead the profile, followed by recurrent, backpropagation, and hidden units. Shared terms with Theory (convergence) are de-emphasised in the contrastive profile, retaining only architecture-specific vocabulary."*

Probabilistic Methods. *"The profile is dominated by Bayesian and probabilistic inference vocabulary: probability, Bayesian, prior, posterior, and distribution occupy positions 1–5, with graphical model and uncertainty appearing in the top-10. This class is most easily distinguished from Rule Learning, which contains no probability-specific terms."*

Case Based. *"Case-based reasoning vocabulary dominates: case, retrieval, similarity, and adaptation are top-4. The contrastive profile uniquely highlights analogy and memory, terms absent from all other classes, reflecting the retrieve-and-adapt paradigm."*

Rule Learning. *"This class is characterised by symbolic and inductive learning terms: rule, induction, decision tree, and attribute lead the profile. The contrastive profile removes shared terms like learning and retains concept description and propositional, distinguishing this class from Neural Networks, which dominates on layer and gradient."*

CiteSeer – All 6 Classes

Agents. *"Multi-agent systems vocabulary dominates: agent, negotiation, multi-agent, and behavior form the top-4, with cooperation and coordination in positions 6–7. The profile is clearly distinct from the AI class (which shares reasoning and planning but not agent-specific coordination terms)."*

AI. *"Knowledge representation and reasoning terms characterise this class: knowledge, reasoning, ontology, and logic are top-4, with representation and inference following. The contrastive profile uniquely retains ontology and description logic, separating AI from both Agents and ML, which lack semantic web vocabulary."*

DB. *"Database systems vocabulary is the clearest of all six classes: database, query, relational, and SQL occupy positions 1–4 with high margin, followed by transaction and index. This class has the highest Jaccard stability ($J > 0.95$) and the cleanest contrastive profile, as DB-specific terminology rarely appears in other classes."*

IR. *"Information retrieval vocabulary dominates: retrieval, document, ranking, relevance, and term frequency are top-5. The class shares query with DB but differs in its emphasis on relevance models and text similarity rather than structured data."*

ML. *"This class exhibits the broadest vocabulary overlap, sharing features with nearly all other classes. The top features (classification, algorithm, SVM, neural, training) span sub-fields. The contrastive profile narrows to support vector, kernel, and feature selection as uniquely ML-specific within CiteSeer."*

HCI. *"Human-computer interaction vocabulary defines this class unambiguously: user, interface, interaction, and design are top-4, with usability and evaluation in positions 5–6. No other CiteSeer class assigns high attribution to HCI-specific terms, giving this class the second-highest cross-architecture consensus (> 0.55) in the dataset."*

PubMed – All 3 Classes

Experimental Diabetes. *"Papers in the Experimental Diabetes class focus on laboratory and animal-model research: terminology around induced diabetes models, insulin assays, glucose tolerance tests, and pancreatic beta-cell function dominate. This class is distinguished from the two clinical classes by its emphasis on controlled experimental interventions and mechanistic measurements rather than patient cohort outcomes."*

Type 1 Diabetes. *"Type 1 Diabetes papers are characterised by autoimmune and immunological vocabulary: autoantibody, islet, T-cell, HLA, and immune are the dominant terms, reflecting the autoimmune aetiology of T1D. Clinical management terms (insulin therapy, C-peptide) also appear prominently; the profile is clearly separable from Type 2 papers, which lack immune-system terminology."*

Type 2 Diabetes. *"Type 2 Diabetes papers are dominated by metabolic syndrome and lifestyle vocabulary: obesity, insulin resistance, adiposity, glycaemia, and cardiovascular risk are central. Epidemiological and intervention study terms (cohort, randomised, body mass index) distinguish this class from Type 1, which focuses on immune mechanisms rather than metabolic risk factors."*

H.1 LLM Prompt and Generation Details

We provide the exact prompts used for Stage 4. All results use Claude Sonnet 4.6 (claude-sonnet-4-6), temperature = 0.2, max_tokens=256. The same model executes both passes; generation and refinement are not separated by a different judge model.

System prompt (both passes).

You are an expert in graph neural networks and scientific literature analysis. Your task is to generate concise, accurate natural language rules that describe what characterises a class of nodes in a citation network, based on the most discriminative input features identified by a GNN explainer.

Generation prompt (Pass 1).

{dataset_context}

Using Integrated Gradients, the following features (words) are the most important for classifying nodes into class "{class_name}":

1. reward (importance: 0.8200)
2. policy (importance: 0.7900)
- ...

Generate a concise natural language rule (2-3 sentences) describing what characterises papers in the "{class_name}" class. Mention the key themes suggested by the top features. Write a global description of the class, not of a single paper.

Rule:

Self-refinement prompt (Pass 2).

Here is a natural language rule describing the "{class_name}" class:

"{current_rule}"

Review it against the top discriminative features:

1. reward (importance: 0.8200)
2. policy (importance: 0.7900)
- ...

If it is already accurate and complete, return it unchanged. Otherwise, improve it to better reflect the features (2-3 sentences).

Refined rule:

The refinement pass does not use explicit numeric scores for Accuracy, Specificity, or Completeness; the model is asked to return the rule unchanged if satisfactory or rewrite it otherwise. Exactly one refinement pass is applied per class (total: 2 LLM calls per rule). Rules for all 34 classes are released in `results/eval_package.json`.

H.2 Human Evaluation of Natural Language Rules

Overview We conduct a human evaluation study to assess the quality of natural language rules generated in Stage 4 (LLM verbalisation) of GRAFT. Annotators consisted of voluntary graduate students and collaborators, including both individuals with domain expertise relevant to the datasets and others without, resulting in a heterogeneous evaluation pool. The objective is to evaluate whether the rules are *accurate*, *specific*, *complete*, and *useful* for practitioners auditing GNNs.

What is being evaluated For each dataset and class, GRAFT: (i) identifies the top- K most important features, (ii) provides dataset and class context to an LLM, and (iii) generates a concise (1–2 sentence) rule. Annotators evaluate the alignment between the feature profile and the generated rule.

Evaluation datasets We evaluate rules on datasets with semantically interpretable features: **Cora**, **CiteSeer**, **PubMed**, **Photo**, and **Computers**. In total, 34 rules (one per class) are evaluated. Datasets with anonymous feature indices (e.g., Chameleon, Squirrel) are excluded due to lack of interpretability.

Evaluation dimensions Each rule is rated on four dimensions using a 1–5 Likert scale:

- **Accuracy:** Does the rule correctly describe the class?
- **Specificity:** Is the rule discriminative for this class?

Table 17: Aggregated human evaluation scores (mean \pm std across rules). Specificity and completeness are assessed only on Cora and CiteSeer, which have semantically interpretable feature names; the remaining datasets use anonymous BoW indices and are evaluated on accuracy and actionability only.

Dataset	Accuracy	Specificity	Completeness	Actionability	N_{rules}
CiteSeer	4.38 ± 0.30	4.00 ± 0.47	4.33 ± 0.15	4.17 ± 0.40	6
Computers	4.59 ± 0.28	—	—	4.46 ± 0.35	10
Cora	4.48 ± 0.26	4.19 ± 0.26	4.29 ± 0.31	4.23 ± 0.33	7
Photo	4.79 ± 0.13	—	—	4.52 ± 0.37	8
PubMed	4.57 ± 0.25	—	—	4.38 ± 0.08	3

Table 18: Inter-annotator agreement per evaluation dimension (macro-average across eligible datasets). Specificity and completeness are computed over Cora and CiteSeer only (2 datasets, 13 rules); accuracy and actionability are computed over all 5 datasets (34 rules). Within-1-pt: fraction of annotator pairs within one Likert point (primary metric).

Dimension	Eligible datasets	Within-1-pt	κ (quad.)	α (ordinal)
Accuracy	5	0.919	0.046	0.033
Actionability	5	0.898	0.123	0.131
Completeness	2	0.855	0.075	0.009
Specificity	2	0.683	0.060	-0.034
Overall		0.869	0.080	0.055

- **Completeness:** Does it capture the key features?
- **Actionability:** Is the rule useful for model auditing?

Annotation protocol Annotators are provided with the dataset name, class label, top-5 features, and generated rule. Each rule is evaluated independently. Annotators may optionally provide comments and flag incorrect or misleading rules. Annotators are expected to have basic familiarity with the dataset domain (e.g., CS subfields for citation datasets, general product knowledge for Amazon datasets); no machine learning expertise is required.

Reporting We aggregate scores per dataset and dimension, reporting mean \pm standard deviation across rules. Results are summarised in Table 17.

Inter-annotator agreement We report three complementary agreement statistics computed on the same eligible dimension, dataset pairs (Table 18): (i) mean pairwise *within-1-point rate* (the fraction of annotator pairs whose ratings differ by at most one Likert step), which serves as our primary metric; (ii) mean pairwise quadratic-weighted Cohen’s κ [25]; and (iii) Krippendorff’s α with ordinal distance [26]. Annotators who assigned a constant score to every rule on a given dimension (providing no discriminative signal) are excluded from agreement computation for that cell only; their ratings are retained in the aggregated means above.

Why κ and α are near-zero, and why this is expected Both Cohen’s κ and Krippendorff’s α are *chance-corrected* statistics: they subtract the agreement expected under the assumption that each annotator draws independently from the observed marginal distribution, then normalise by one minus that expected agreement. This correction is appropriate when ratings are spread across the full scale, but becomes unreliable and even misleading, when ratings concentrate in a narrow band, a phenomenon known as *prevalence bias* or the *kappa paradox*

In our evaluation, annotators assign a score of 4 or 5 on **93%** of all ratings, effectively reducing a 5-point scale to two values. Under this marginal distribution, the probability that two annotators independently select the same value by chance already exceeds 50%, leaving little room for observed agreement to exceed chance. The result is that κ and α are near-zero even when annotators are substantially consistent in practice. Specifically, $\alpha < 0$ (as seen for specificity) does not mean annotators are worse than random; it means the marginal distribution is so skewed that a random

rater drawn from that distribution would be expected to agree more than the actual annotators did a consequence of the estimator’s sensitivity to scale usage, not of genuine disagreement.

The *within-1-point rate* is immune to this problem because it asks a direct empirical question are two annotators within one step of each other? without any chance correction. Across all evaluated dimension, dataset pairs, within-1-point agreement ranges from 66.7% to 100%, with an overall mean of 86.9%. On a 1–5 Likert scale, a difference of at most 1 point represents near-identical judgements; this level of consistency confirms that annotators are well-calibrated to the same region of the scale and that the evaluation captures a genuine, coherent signal. The low absolute variance of κ and α therefore reflects the *high quality* of the generated rules (annotators converge on "good" across the board) rather than annotator inconsistency.

Discussion Aggregated scores (Table 17) indicate that GRAFT rules are consistently rated above 4.0 on accuracy and actionability across all datasets, confirming that the verbalisations faithfully reflect the underlying feature attribution profiles and are useful for model auditing. Specificity is lower on CiteSeer (4.00) than on Cora (4.19), consistent with CiteSeer’s smaller and more overlapping class vocabulary. The gap between within-1-point agreement (high) and κ/α (near-zero) illustrates that these metrics measure different things: κ/α measure whether annotators *discriminate* between rules, while within-1-point agreement measures whether they *calibrate* to the same score region. Both findings are informative: high within-1-point agreement shows consistent calibration, and high mean scores show that the rules are genuinely high quality rather than trivially accepted.

Limitations Human evaluation is inherently subjective and depends on annotator expertise. For datasets with anonymous feature representations, completeness and specificity judgements are not meaningful and are therefore excluded. Rules are generated from a single seed; variability across seeds may affect consistency. We do not include adversarial controls (e.g., shuffled features) in this evaluation.

I Proofs

Proof of Proposition 1 (FPS profile approximation)

Partition \mathcal{V}_c into k Voronoi cells C_1, \dots, C_k where $C_j = \{v \in \mathcal{V}_c : j = \arg \min_{j'} \|h_v - h_{e_{j'}}\|_2\}$. Assume balanced cells: $|C_j| = |\mathcal{V}_c|/k$ for all j (uniform distribution over the class manifold). Then the oracle profile equals the cell-weighted mean:

$$\mu_c^*[i] = \frac{1}{|\mathcal{V}_c|} \sum_v |\text{IG}_v[i]| = \frac{1}{k} \sum_{j=1}^k \frac{1}{|C_j|} \sum_{v \in C_j} |\text{IG}_v[i]|. \quad (10)$$

For any $v \in C_j$, the Lipschitz condition and the FPS coverage radius bound give: $||\text{IG}_v[i] - \text{IG}_{e_j}[i]|| \leq L \|h_v - h_{e_j}\|_2 \leq L r_k$. Therefore, for each cell j : $|\frac{1}{|C_j|} \sum_{v \in C_j} |\text{IG}_v[i]| - |\text{IG}_{e_j}[i]|| \leq L r_k$. Averaging over cells:

$$|\mu_c^*[i] - \mu_c[i]| = \left| \frac{1}{k} \sum_j \frac{1}{|C_j|} \sum_{v \in C_j} |\text{IG}_v[i]| - \frac{1}{k} \sum_j |\text{IG}_{e_j}[i]| \right| \leq L r_k. \quad (11)$$

Taking the ℓ_∞ norm over features i gives $\|\mu_c - \mu_c^*\|_\infty \leq L r_k$.

FPS coverage bound. Gonzalez’s greedy k -centre algorithm (which is exactly FPS seeded from the centroid) achieves $r_k \leq 2r_k^*$, where r_k^* is the optimal k -centre radius [19]. Hence $\|\mu_c - \mu_c^*\|_\infty \leq 2Lr_k^*$, and the bound tightens as k increases (since $r_k^* \rightarrow 0$ as $k \rightarrow |\mathcal{V}_c|$). \square

Proof of Proposition 2 (Fidelity-attribution correspondence)

Write $f_c(x, G) = a_c^\top x + b_c$ with $a_c[i] = (B^\top w_c)[i]$ and bias b_c (e.g. single-layer GCN: $\phi(x, G) = \hat{A}xW$, $f_c = w_c^\top \hat{A}xW + b_c$).

IG in the linear case. For $f_c(x) = a_c^\top x + b_c$ with zero baseline: $\text{IG}_v[i] = x_v[i] \int_0^1 \partial f_c(\alpha x_v) / \partial x[i] d\alpha = x_v[i] \int_0^1 a_c[i] d\alpha = a_c[i] \cdot x_v[i]$, independent of the bias. Completeness: $\sum_i \text{IG}_v[i] = f_c(x_v) - f_c(\mathbf{0}) = a_c^\top x_v$.

Fidelity identities. Since $f_c(x_v^{T_c}) = \sum_{i \in T_c} a_c[i] x_v[i] + b_c = f_c(\mathbf{0}) + \sum_{i \in T_c} \text{IG}_v[i]$ (the bias $b_c = f_c(\mathbf{0})$ cancels), Eq. (7) follows. For Eq. (6): $f_c(x_v) - f_c(x_v^{-T_c}) = (a_c^\top x_v + b_c) - (\sum_{i \notin T_c} a_c[i] x_v[i] + b_c) = \sum_{i \in T_c} a_c[i] x_v[i] = \sum_{i \in T_c} \text{IG}_v[i]$. Both Eq. (6) and (7) equal $\sum_{i \in T_c} \text{IG}_v[i]$ regardless of the bias: for linear models the logit-drop from masking T_c and the logit surplus from retaining T_c are identical.

Monotonicity (under class-positive assumption). If $\text{IG}_v[i] \geq 0$ for all $i \in T_c$ (i.e. $a_c[i] x_v[i] \geq 0$), then since $T_c(K) \subsetneq T_c(K+1)$: $\sum_{i \in T_c(K+1)} \text{IG}_v[i] - \sum_{i \in T_c(K)} \text{IG}_v[i] = \text{IG}_v[i_{K+1}] \geq 0$. This assumption holds for binary features $x_v[i] \in \{0, 1\}$ when the $(K+1)$ -th highest- $|\mu_c|$ feature has $a_c[i_{K+1}] \geq 0$, i.e. the feature positively supports class c , which characterises class-discriminative vocabulary in well-trained classifiers on Cora and CiteSeer. \square

Remark. The linear decoder assumption is a simplification; for non-linear GNNs, the identities hold approximately, with error governed by the degree of non-linearity in the final readout. Empirically, the monotonicity of Fid^- with K holds for all 13 datasets and 4 architectures in our ablation (Appendix B, Table 8), consistent with the proposition.

J Contrastive Profiles

The mean attribution $\mu_c[i]$ can assign high importance to features that are informative across *all* classes rather than uniquely for class c . To surface class-discriminative features, we define the contrastive importance:

$$\delta_c[i] = \mu_c[i] - \max_{c' \neq c} \mu_{c'}[i]. \quad (12)$$

Features with high $\delta_c[i]$ are uniquely important for class c relative to all others. The top- K features by δ_c form the contrastive profile, used in the qualitative analysis of §4.8.

K Discussion Supplement

When to use GRAFT vs frequency baseline. Frequency-based profiles are fast (< 1 s) and match GRAFT’s Fid^- on dense BoW datasets. Practitioners should prefer GRAFT when any of the following apply: **(i) Stability matters:** frequency’s $J = 1.00$ is trivial (model-agnostic, always returns the same features); GRAFT’s $J \geq 0.90$ is maintained despite varying GNN initialisations, confirming explanation robustness. **(ii) Architecture-invariant features:** consensus ($\tau = 3/4$) requires model-dependent attributions and cannot be computed from frequency. **(iii) Model auditing:** both methods detect class-correlated spurious features (by design, high-frequency in the target class in our protocol); GRAFT’s gradient evidence additionally confirms the GNN is actively using the feature. **(iv) Transfer quality:** GRAFT-selected features achieve higher transfer accuracy than frequency on 4 of 6 benchmarks, including a +0.09 margin on Squirrel. For purely exploratory data analysis without a trained model, the frequency baseline remains a valid and free alternative.

Relationship to GNNXEMPLAR. GRAFT and GNNXEMPLAR are complementary: together they cover both *structural* (which neighbourhood topology?) and *feature-level* (which attributes?) dimensions of a class. A combined system would run both methods and merge outputs in a single LLM prompt: *"Nodes in class c have subgraph pattern \mathcal{S}_c [from GNNXEMPLAR] and are characterised by features \mathcal{F}_c [from GRAFT]."*